18th International Conference on Information Fusion
Washington, DC - July 6-9, 2015

Cubature/ Unscented/ Sigma Point Kalman Filtering with Angular Measurement Models

David Frederic Crouse
Naval Research Laboratory
4555 Overlook Ave., SW
Washington DC 20375
E-Mail: david.crouse@nrl.navy.mil

***Abstract*—Filtering algorithms that use different forms of numerical integration to handle measurement and process nonlinearities, such as the cubature Kalman filter, can perform extremely poorly in many applications involving angular measurements. We demonstrate how such filters can be modified to take into account the circular nature of the angular measurements, dramatically improving performance. Unlike common alternate techniques, the cubature methods can be easily used with angular measurements arising from ray-traceable propagation models.**

I. Introduction

The recent tutorial [9] discusses, considering examples of 3D target tracking, how cubature/ unscented/ sigma point Kalman filtering is a realization of the best linear unbiased estimator (BLUE) that evaluates certain integrals for expected values using different forms of cubature integration. In [9], the term "cubature Kalman filter" is generally applied to all such filters to highlight the use of cubature integration,[1] whereas in [28] the term "linear regression Kalman filter" is used to highlight how such methods can be viewed as a form of linear regression. This paper addresses the use of the generic family of all cubature Kalman filters[2] (CKFs) with measurement and dynamic models involving angular components without regard to the choice of cubature points.

Though many articles on various types of cubature Kalman filters (CKFs) consider the use of polar [20], [12], [2] or spherical [34] measurements with Cartesian state vectors, many more papers that consider the use of cubature integration (usually in the form of the "unscented transform") consider just converting such measurements into Cartesian coordinates and feeding the converted measurements to a standard linear Kalman filter, such as in [19], [20], [17], [18], [1], [32]. However, in [9], it was demonstrated that when tracking using range and direction cosine measurements, it is better to use them in a CKF than to to use unbiased Cartesian-converted measurements for tracking and one would expect similar results to hold when using measurements in spherical coordinates.

[1]Sometimes the term "quadrature" is used in place of cubature. Usually, the distinction is the quadrature integration is one-dimensional, whereas cubature integration is multidimensional. However, not all authors make the distinction.

[2]The term "cubature Kalman filter" was coined in the paper [2], where third-order cubature points were used. Many authors, when discussing the CKF only mean the CKF with that particular choice of cubature points.

However, none of the aforementioned papers considering the use of polar or spherical coordinates in a CKF takes into consideration the idiosyncrasies of directional statistics. In various monographs on directional statistics [30] focussing on circular [13] or spherical [14] measurements, problems with traditional definitions of the mean and variance are highlighted. For example, in numerous examples throughout [13], the problem of averaging wind directions (in the local tangent plane to the surface of the Earth) is considered. If one were to simply numerically average the direction (given as an angle, for example, North of East or East of North), then averaging a value just above 0° with one just below 359° would produce the worst possible estimate, one close to 180° –exactly opposite the direction of both of the samples. Thus, special care must be taken when computing expected values involving numerical data. Consequently, as is demonstrated for polar measurements in Section III, and spherical measurements in Section IV, special care must be taken when computing the expected values in the CKF when dealing with angular models.

Directional statistics have been used in various aspects of filtering in the past. For example, in [26], the measurement update step of a particle filter whose target state vector contains an angular component is considered. In [36], parts of a standard Kalman filter used to estimate angular distributions are wrapped on the range $(0, 2\pi]$ to handle special nonlinear aspects of the filter. The same concept is applied in this paper to the more general CKF problems. On the other hand, a cubature-style filter is used with the wrapped-normal and von Mises distributions for estimating an angle in [25]. In [24], the authors consider the more general case where multiple angles are dependent, such as when using spherical coordinates, where toroidal distributions and moments were used. Though the algorithms of [25] and [24] work quite well when estimating angular quantities, this paper considers more general estimation problems when given correlated quantities other than angles, for example, problems involving range or Cartesian position in the state and/ or the measurement vectors. Whereas in [25], [24], solutions utilizing circular probability distributions are derived, this paper simply demonstrates how a standard linear CKF can be modified to accommodate circular or spherical models when the noises involved are not "too"

large.

Though the CKF is not suitable for all estimation problems, it is extremely versatile and simple to use in many challenging scenarios. For example, in the tutorial [8], it is demonstrated that the CKF can handle refraction-corrupted measurements well in ray-traceable atmospheric models without having to evaluate derivatives. Additionally, since the measurement propagation and update steps in the CKF are separate, one can easily be replaced by another algorithm utilizing Gaussian approximations. For example, in the tutorial [7], the CKF measurement update step is paired with a cubature-based moment-matching method for propagating a target state through a nonlinear stochastic dynamic model with non-additive noise, as opposed to the derivative-based nonlinear state propagation algorithm introduced in [3].

Section II reviews basic aspects of the measurement update step common to CKF that are discussed in detail in [9]. Sections III and IV then discuss how the CKF measurement update step can be modified to handle polar and spherical measurements, respectively. The results are summarized in Section V.

II. The Basic Form of Cubature Kalman Filters

As discussed in [9], cubature integration is based on the Fundamental Theorem of Gaussian Integration, which states that the definite integral of any polynomial up to a given degree times a weighting function w having certain properties can be determined exactly by a weighted summation of the polynomial evaluated at certain fixed points based on the weighting function. As an equation, for a scalar integral, this means that

$$\int_a^b w(x)g(x)\,dx = \sum_{i=0}^{n} \omega_i g(\xi_i), \tag{1}$$

where a and b are the bounds of the integral, $w(x)$ is the weighting function, $g(x)$ is a polynomial, ω_i is a cubature weight and ξ_i is a cubature point (sometimes referred to as a sigma-point in tracking literature). The cubature points and weights are designed to be valid for all polynomials up to a certain degree. For polynomials over that degree, the integration can only be considered an approximation.

A monograph by Stroud [35][3] discusses aspects of cubature integration for many different weighting functions and regions of integration. Common scalar weighting functions for d-dimensional multivariate integrals in $\mathbb{R}$ are $w(\mathbf{x}) = e^{\|\mathbf{x}\|}$ and $w(\mathbf{x}) = e^{\|\mathbf{x}\|^2}$. When $w(\mathbf{x}) = 1$, common regions of integration are the unit sphere (or hypersphere in more than 3 dimensions), cube (or hypercube), and simplex (a triangle in 2D, a tetrahedron in 3D, and similar shapes in higher dimensions). As demonstrated in [9], cubature formulae for the weighting function $w(\mathbf{x}) = e^{\|\mathbf{x}\|^2}$ can be modified to work for scenarios when one is performing an integral of a function times a multivariate normal PDF having an arbitrary mean and covariance. In other words, when dealing with integrals that arise when deriving the CKF.[4]

Mathematicians have developed numerous cubature formulae as tabulated in [35] and in the online encyclopedia of cubature formulae at http://nines.cs.kuleuven.be/ecf/ described in [6]. Many versions of the CKF use cubature integration without having derived it from the mathetical literature on the topic. For example, while the formula underlying Arasaratnam and Haykin's CKF [2] is a third-order cubature formula, which was derived with regard to the mathematical literature on cubature integration, the so-called "unscented transformation" in the unscented Kalman filter [21], [16], [27] is a third-order cubature formula that was derived independently of past mathematical work, Similarly, the recent smart sampling Kalman filter [33] uses a stochastic method to choose points for integration that are de facto cubature points.

The key to the CKF is the update step, which is an implementation of the best linear unbiased estimator (BLUE) using cubature integration to evaluate difficult integrals. The BLUE is described in the context of target tracking (but not cubature integration) in [38], where solutions for tracking using polar measurements and using spherical measurements are given using a Taylor-series approximation assuming that no correlation exists between the noise corrupting the components of the measurement. In practice, however, recursion is not necessary as the algorithm is shown to perform well against other techniques in [22].

On the other hand, a cubature-based BLUE can handle more general scenarios, such as when correlation between the components of measurements is taken into account or when using empirical models of range-Doppler coupling, such as the model of [5]. The estimation step in the BLUE/ CKF is

$$\hat{\mathbf{x}}_{k|k} = \hat{\mathbf{x}}_{k|k-1} + \overbrace{\mathbf{P}^{xz}_{k|k-1}\left(\mathbf{P}^{zz}_{k|k-1}\right)^{-1}}^{\mathbf{W}_k}\left(\mathbf{z}_k - \hat{\mathbf{z}}_{k|k-1}\right), \tag{2}$$

$$\mathbf{P}_{k|k} = \mathbf{P}_{k|k-1} - \mathbf{P}^{xz}_{k|k-1}\left(\mathbf{P}^{zz}_{k|k-1}\right)^{-1}\left(\mathbf{P}^{xz}_{k|k-1}\right)', \tag{3}$$

where $\hat{\mathbf{x}}_{k|k-1}$ is the predicted (prior mean) target state with covariance matrix $\mathbf{P}_{k|k-1}$ (a Gaussian distribution is assumed) and $\hat{\mathbf{x}}_{k|k}$ is the updated (posterior mean) target state with covariance matrix $\mathbf{P}_{k|k}$. $\mathbf{z}_k$ is the measurement, and the term $\mathbf{W}_k$ is known as the "gain" of the filter. The other quantities are given in terms of expected values as

$$\hat{\mathbf{z}}_{k|k-1} = \mathrm{E}\left[h(\mathbf{x}_k, \mathbf{w}_k) \middle| \mathbf{Z}_{1:(k-1)}\right], \tag{4}$$

$$\mathbf{P}^{xz}_{k|k-1} = \mathrm{E}\left[\left(\mathbf{x}_k - \hat{\mathbf{x}}_{k|k-1}\right)\left(\mathbf{z}_k - \hat{\mathbf{z}}_{k|k-1}\right)' \middle| \mathbf{Z}_{1:(k-1)}\right], \tag{5}$$

$$\mathbf{P}^{zz}_{k|k-1} = \mathrm{E}\left[\left(\mathbf{z}_k - \hat{\mathbf{z}}_{k|k-1}\right)\left(\mathbf{z}_k - \hat{\mathbf{z}}_{k|k-1}\right)' \middle| \mathbf{Z}_{1:(k-1)}\right], \tag{6}$$

[3] Stroud's extensive monograph on cubature integration [35] is out of print. Since the book was printed in 1971 and U.S copyright on a work published in 1971 is valid 95 years from the copyright date [37], the copyright will not expire until 2066.

[4] Cubature formulae for the weighting function $w(\mathbf{x}) = e^{\|\mathbf{x}\|}$ could be similarly transformed to work with the Laplace distribution. Cubature formulae for $w(\mathbf{x}) = 1$ over regions of various shapes could be used for evaluating polynomial integrals over uniform distributions of various shapes.

where the conditioning $\mathbf{Z}_{1:(k-1)}$ is on all prior information (which is assumed to result in a Gaussian prior distribution), and $h(\mathbf{x}_k, \mathbf{w}_k)$ is the function that transforms that state $\mathbf{x}_k$ into the measurement, including Gaussian measurement noise $\mathbf{w}_k$, which could be additive or included in a nonlinear manner. To simplify the discussion in this paper, the measurement noise is assumed additive. That is $h(\mathbf{x}_k) + \mathbf{w}_k$ is used in place of $h(\mathbf{x}_k, \mathbf{w}_k)$. However, the concepts of this paper can be applied to general noise models as in Section IX.C of [9]. In [38], the BLUE problem is formulated slightly differently so that the measurement is converted into the target state (Cartesian) domain, whereas here, $\hat{\mathbf{z}}_{k|k-1}$ is the conversion of the target state into the measurement domain.

Though cubature estimation techniques have been developed for circular probability distributions such as in [23], there are no cubature estimation methods explicitly for measurement models where only some of the components of the measurement are circular, such as when given a range and an azimuth measurement. Thus, this paper demonstrates how linear models can be adapted to such applications.

Note that the assumption that the noise corrupting the measurement is Gaussian-distributed is kept here. Strictly speaking, the assumption regarding noise corrupting the angular component is best described as wrapped normal, which is described in [30, Ch. 3.5.7]. By approximating the noise corrupting the measurement as being multivariate normal, it is possible to approximately model cross-correlations between angular and linear components. Also note that if the noise variance on the angular component is small, standard methods (possibly modified with a modulo operation) can be used to approximately estimate the covariance matrix of the measurements from measurement and truth data. This becomes clear when examining the (scalar) clipped mod normal distribution used in [11], which differs very little from a standard normal distribution, but which can be applied to circular data without explicit wrapping.

III. Using Polar Measurement in a Cubature Filter

A. The Method

In the standard CKF, one would expect problems to arise when taking the differences of the angular components in (2) when computing $\hat{\mathbf{x}}_{k|k}$, as well as in (5) and (6), when computing $\mathbf{P}^{xz}_{k|k-1}$ and $\mathbf{P}^{zz}_{k|k-1}$, due to the difference between angles being discontinuous at the $0 - 2\pi$ boundary in the angular components of the innovation term $\mathbf{z}_k - \hat{\mathbf{z}}_{k|k-1}$ and the $\mathbf{z} - \hat{\mathbf{z}}_{k|k-1}$ terms. Additionally, the evaluation of the expected value in (4) to compute the predicted measurements involves a conversion of the target state into the coordinate system of the measurement. When given measurements in polar coordinates and a target state in Cartesian coordinates, however, problems related to averaging angles can arise.

When finding the mean and variance of circular values, the mean direction μ_θ is typically used in place of the arithmetic mean and the circular variance σ^2_θ in place of the more traditional standard deviation. Given an angle θ, the mean direction and circular standard deviation are generally defined in terms of average components $\bar{u}_x$ and $\bar{u}_y$ of an algebraic average of unit vectors[5] $\bar{\mathbf{u}}$ as well as the mean resultant length, ρ such that

$$\bar{u}_x \triangleq \mathrm{E}\left[\cos\theta\right] \qquad \bar{u}_y \triangleq \mathrm{E}\left[\sin\theta\right]. \tag{7}$$

The mean resultant length, ρ, and mean direction, μ_θ, are defined through the polar relation [30, Ch. 2.2]

$$\bar{u}_x + j\bar{u}_y = \rho e^{j\mu_\theta}, \tag{8}$$

where $j = \sqrt{-1}$. Thus,

$$\rho \triangleq \sqrt{\bar{u}_y^2 + \bar{u}_x^2} \qquad \mu_\theta \triangleq \arctan2\left(\bar{u}_y, \bar{u}_x\right), \tag{9}$$

where $\arctan2$ refers to a four-quadrant inverse tangent function. The circular standard deviation is defined as [30, Ch. 2.3]

$$\sigma^2_\theta \triangleq -2\ln\rho \tag{10}$$

When deriving an angle-only recursive filtering algorithm in [25], the authors made use of such circular statistics in the context of circular probability distributions. However, here, we consider the more general problem of handing both linear (range) and circular (angle) measurement components, which could possibly be correlated. In [30, Ch. 11.1], the concept of a cross correlation between circular and linear terms is defined and in [30, Ch. 11.3] the topic of performing regression between circular and linear quantities is broached. However, the regression technique is not sufficiently well developed to completely replace the CKF and it would be inappropriate to replace $\mathbf{P}^{zz}_{k|k-1}$ and $\mathbf{P}^{xz}_{k|k-1}$ with components having fully circular terms as long as the design of the overall measurement update remained linear.

Even though a version of the CKF for mixed circular and linear variables is not trivial to derive, one can assume that a simple modification to a linear estimator would work well. For example, in [10], when considering range ambiguity resolution, which results from aliasing in range measurements (a circular property), it is demonstrated that a simple algorithm based on a linear model works nearly as well as an optimal algorithm, because there is not much noise in a realistic system. In the problem at hand here, simple *ad-hoc* corrections to eliminate the $0-2\pi$ discontinuity can eliminate any problems.

Thus, the expected value in (4) is not implemented in the traditional manner described in [9], which is

$$\hat{\mathbf{z}}_{k|k-1} = \sum_{i=0}^{N_C} \omega_i \boldsymbol{\zeta}^z_i, \tag{11}$$

where

$$\boldsymbol{\zeta}^z_i = h(\hat{\mathbf{x}}_{k|k-1} + \mathbf{P}^{\frac{1}{2}}_{k|k-1}\boldsymbol{\zeta}_i) \tag{12}$$

is the ith cubature weight out of a total of N_c that has been transformed to model the moments of the noisy target state after measurement prediction, and the matrix square root in

[5]The algebraic mean of unit vectors is usually not a unit vector.

(12) should be a lower-triangular Cholesky decomposition. Rather, if the measurement function contains a circular component, then that has to be averaged separately from the other components in the manner of (9). Note that in (12), h is the polar measurement function

$$h(\mathbf{x}) = [\sqrt{x^2+y^2}, \operatorname{arctan2}(y,x)]'. \tag{13}$$

For the case where one has 2D range and position components the steps are

1) Compute cubature points for the distribution of the predicted measurement in the manner normally done for cubature integration. That is, use (12). The cubature point $\boldsymbol{\zeta}_i^z = [\zeta_i^{z,r}, \zeta_i^{z,\theta}]'$ is composed of a range component $\zeta_i^{z,r}$ and an angular component $\zeta_i^{z,\theta}$.
2) The mean of the range components is found the standard way as a linear sum

$$\hat{z}_{k|k-1}^r = \sum_{i=0}^{N_C} \omega_i \zeta_i^{z,r}. \tag{14}$$

3) The mean angular component, on the other hand, is the weighted average of the direction vectors (the sample mean)

$$\mathbf{u}_i = \begin{bmatrix} \cos\left(\zeta_i^{z,\theta}\right) \\ \sin\left(\zeta_i^{z,\theta}\right) \end{bmatrix}, \tag{15}$$

$$\bar{\mathbf{u}} = \sum_{i=0}^{N_C} \omega_i \mathbf{u}_i. \tag{16}$$

$$\hat{z}_{k|k-1}^\theta = \operatorname{arctan2}\left(u_y, u_x\right). \tag{17}$$

In other words, the cubature integration is used to approximately evaluate the integrals in (7).
4) The predicted measurement is now $\hat{\mathbf{z}}_{k|k-1} = [\hat{z}_{k|k-1}^r, \hat{z}_{k|k-1}^\theta]'$.

On the other hand, when evaluating the innovation term $\mathbf{z}_k - \hat{\mathbf{z}}_{k|k-1}$ in (2), as well the angular differences in(5), (6) for $\mathbf{P}_{k|k-1}^{xz}$ and $\mathbf{P}_{k|k-1}^{zz}$ via cubature integration, an *ad-hoc* method of dealing with the circular nature of the azimuth component of the measurement is to realize that all differences between angles must be bound between $\pm\pi$. Thus, all differences between angles should be wrapped into that region. To wrap a value to the region (a,b), where $a < b$, one can use the function

$$h^{\text{wrap}}(x,a,b) = \operatorname{mod}(x-a, b-a) + a, \tag{18}$$

where mod refers to the modulo operation (the `mod` function in Matlab). For example, $\operatorname{mod}(12,5) = 2$. Thus, equation (2) becomes

$$\hat{\mathbf{x}}_{k|k} = \hat{\mathbf{x}}_{k|k-1} + \mathbf{P}_{k|k-1}^{xz} \left(\mathbf{P}_{k|k-1}^{zz}\right)^{-1} h_{\text{polar}}^{\text{wrap}}\left(\mathbf{z}_k - \hat{\mathbf{z}}_{k|k-1}\right), \tag{19}$$

where for some difference parameter $\Delta\mathbf{z} = [\Delta r, \Delta\theta]'$,

$$h_{\text{polar}}^{\text{wrap}}(\Delta\mathbf{z}) = \begin{bmatrix} \Delta r \\ h^{\text{wrap}}(\Delta\theta, -\pi, \pi) \end{bmatrix}. \tag{20}$$

Using the wrapping function $h_{\text{polar}}^{\text{wrap}}$, (5) and (6) are similarly evaluated as

1) Compute cubature points for the distribution of the predicted state in the manner normally done for cubature integration. That is, use (12) to get $\boldsymbol{\zeta}_i^z = [\zeta_i^{z,r}, \zeta_i^{z,\theta}]'$. Also, save the non-transformed cubature points,

$$\boldsymbol{\zeta}_i^x = \hat{\mathbf{x}}_{k|k-1} + \mathbf{P}_{k|k-1}^{\frac{1}{2}} \boldsymbol{\zeta}_i. \tag{21}$$

2) $\mathbf{P}_{k|k-1}^{xz}$ and $\mathbf{P}_{k|k-1}^{zz}$ are evaluated as

$$\mathbf{P}_{k|k-1}^{xz} = \sum_{i=0}^{N_C-1} \omega_i \left(\boldsymbol{\zeta}_i^x - \hat{\mathbf{x}}_{k|k-1}\right) h_{\text{polar}}^{\text{wrap}}\left(\boldsymbol{\zeta}_i^z - \hat{\mathbf{z}}_{k|k-1}, -\pi, \pi\right)', \tag{22}$$

$$\mathbf{P}_{k|k-1}^{zz} = \sum_{i=0}^{N_C-1} \omega_i h_{\text{polar}}^{\text{wrap}}\left(\boldsymbol{\zeta}_i^z - \hat{\mathbf{z}}_{k|k-1}\right) h_{\text{polar}}^{\text{wrap}}\left(\boldsymbol{\zeta}_i^z - \hat{\mathbf{z}}_{k|k-1}\right)'. \tag{23}$$

B. An Example

As an example, consider the problem of tracking a target moving with a nearly-constant velocity in two dimensions. This is a 2D order-1 version of the generalized model given in Appendix A. Under this model the target state has the form $\mathbf{x} = [x, y, \dot{x}, \dot{y}]'$ for 2D position (x, y) and velocity $(\dot{x}, \dot{y})$ components.

Two scenarios are considered. The initial target states in the scenarios are

$$\mathbf{x}_0^{(0)} = \begin{bmatrix} 100\,\text{km} & 0 & -200\,\text{m/s} & 0 \end{bmatrix}', \tag{24}$$

$$\mathbf{x}_0^{(1)} = \begin{bmatrix} -100\,\text{km} & 0 & 200\,\text{m/s} & 0 \end{bmatrix}'. \tag{25}$$

In both instances, the target is heading toward the origin (where the sensor is located), but the target is on either side of the y-axis. For polar measurements, where the range ranges $\pm\pi$ measured counterclockwise from the x-axis, this means that one would expect the traditional CKF to have significant problems with the track having initial state $\mathbf{x}_0^{(1)}$.

The simulations are run assuming that the components of the Gaussian noise corrupting the range and angle measurements are uncorrelated with range standard deviation $\sigma_r = 20\,\text{m}$ and angular standard deviation $\sigma_\theta = 0.5°$. The time between measurements is a constant $T = 3\,\text{s}$. The process noise intensity parameter is $q = 1\,\text{m}^2/\text{s}^3$.

The simulation is run using four filters. The first is a standard Kalman filter, which uses uses the first-two moments of the Cartesian converted measurements computed using ninth-order cubature integration, as done is in [9]. However, since the fifth-order cubature relations given in [9] require points to have three or more dimensions, the arbitrary-order 1-dimensional routine of [15] is used with the product rule of [35, Ch. 2] to make it two-dimensional. The second filter is the approximate

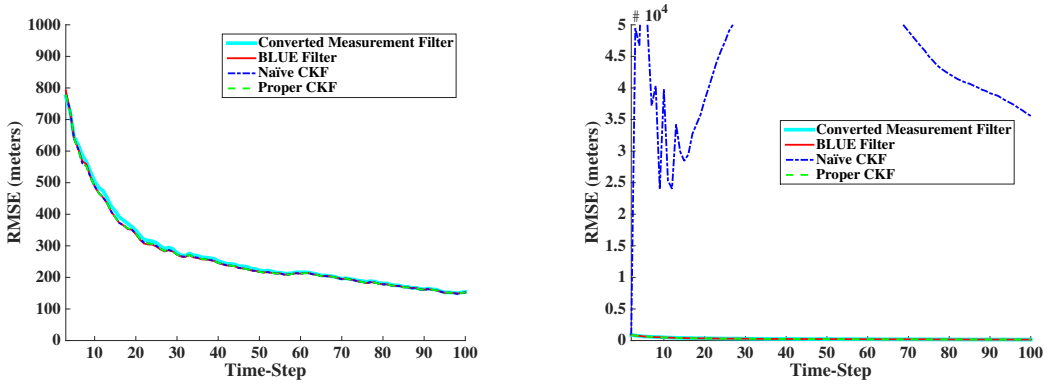

(a) RMSE Using $\mathbf{x}_0^{(0)}$ (b) RMSE Using $\mathbf{x}_0^{(1)}$

Fig. 1. A comparison of the different filtering algorithms. In (a) and (b) the RMSE performance of the different filtering algorithms is shown. In (a), where the initial target state is on the right of the y-axis, far from the $\pm\pi$ boundary in polar angle, all of the filters perform similarly, though if plotted, one would see that the average normalized estimation error squared (ANEES) performance of the converted measurement filter is somewhat less statistically consistent. However, in (b), where the initial target state is on the left of the y axis, near the $\pm\pi$ boundary, the performance of naïve CKF is extremely poor. Observing a sample Monte Carlo run, one would see that the naïve filter experiences wild gyrations; the proper CKF implementation of this paper does not.

BLUE filter of [38], which avoids problems with angles by performing the measurement update step with a different formulation using Cartesian coordinates. The third filter is a naïve CKF with ninth-order cubature points, implemented as described in [9] without accounting for the circular nature of the measurements. The fourth filter is a "proper" CKF, which has been adjusted as described in this paper to avoid problems with measurements near a $\pm\pi$ boundary. The two implementations of the CKF use the same fifth-order cubature points as used in the simulations in [9].

Figures 1a and 1b show the root-mean-squared error performance of the filters in the two different scenarios. In 1a, when all of the filters are far from the $\pm\pi$ boundary, the performance is comparable, though the average normalized estimation errors squared (ANEES) of the filters (a measure of the consistency of the covariance matrix with actually observed error, discussed in [9])[6] are comparable, except for the converted measurement filter, which more frequently leaves the 95% confidence interval (not plotted).

In 1b, when near the boundary, the naïve CKF has extremely poor performance. Viewing a sample Monte Carlo of the poor scenario in Figure 1, one would see that the naïve CKF has wild jumps. On the other hand, when far from the boundary, the performance of the filters is comparable.

The proper CKF avoid the problems of the naïve CKF having comparable performance and statistical consistency as the approximate BLUE estimator of [38]. However, it should be noted that unlike the BLUE estimator of [38], the CKF can be used with polar measurements originating from *other* propagation models. That is, the measurement function in the filter can include some type of ray tracing or other effects. For example, the measurement could consist of a 2D bistatic range and angle. The filter of [38] has only been formulated for the monostatic, refraction-free scenario.

[6]The ANEES is a less reliable measure of the accuracy of a covariance matrix than the noncredibility index and the inclination indicator of [29], but it is easier to understand at a glance than using two different measures.

IV. Using Spherical Measurements in a Cubature Filter

A. The Method

When given measurements in spherical coordinates, the same approach as in Section III-A is taken to approximate the integrals in (4), (5), and (6) and to deal with the differencing of direction components in (2). That is, find the average direction instead of the linear mean, when averaging angular components to get $\hat{\mathbf{z}}_{k|k-1}$, and wrap all differences between angles to the appropriate region in spherical space.

The evaluation of $\hat{\mathbf{z}}_{k|k-1}$ is straightforward since the average direction in spherical coordinates is a weighted set of unit vectors. Note, however, that the computation of the unit vector varies depending on how spherical coordinates are defined. For example, a common representation of a point in spherical coordinates is (r, θ, ϕ), where θ is an azimuth measured in the $x-y$ plane, as radians counterclockwise from the x axis and ϕ is an elevation above the plane. In such an instance, the equations for a point (x, y, z) in Cartesian space given a point in spherical coordinates is

$$x = r\cos(\theta)\cos(\phi) \quad y = r\sin(\theta)\cos(\phi) \quad z = r\sin(\phi). \tag{26}$$

The inverse transformation is consequently,

$$r = \sqrt{x^2+y^2+z^2} \quad \theta = \arctan 2\,(y, x) \quad \phi = \arcsin\left(\frac{z}{r}\right). \tag{27}$$

To find unit vectors for averaging, it given a Cartesian state with position components $\mathbf{x}_p = [x, y, z]'$, a unit vector $\mathbf{u}^p$ is simply

$$\mathbf{u}^p = \frac{\mathbf{x}_p}{\|\mathbf{x}_p\|}. \tag{28}$$

When given angular components, a unit vector $\mathbf{u}^\theta$ can be found by evaluating (26) with $r = 1$.

The steps to find $\hat{\mathbf{z}}_{k|k-1}$ are consequently,

1) Compute the transformed cubature points $\boldsymbol{\zeta}_i^z = [\zeta_i^{z,r}, \mathbf{u}_i^z]'$ using (12), where the function h computes the range as in the transformation from Cartesian to spherical coordinates in (27), but the unit direction vector is computed using with the position components of the cubature point 28.
2) The mean of the range components is found the standard way as a linear sum,

$$\hat{z}_{k|k-1}^r = \sum_{i=0}^{N_C} \omega_i \zeta_i^{z,r}. \tag{29}$$

3) Average 3D unit vectors for all of the cubature points:

$$\bar{\mathbf{u}} = \sum_{i=0}^{N_C} \omega_i \mathbf{u}_i^z, \tag{30}$$

$$\hat{z}_{k|k-1}^\theta = \arctan 2\left(\bar{u}_y, \bar{u}_x\right), \tag{31}$$

$$\hat{z}_{k|k-1}^\phi = \arcsin\left(\frac{\bar{u}_z}{\|\bar{\mathbf{u}}\|}\right). \tag{32}$$

where $\bar{\mathbf{u}} = [\bar{u}_x, \bar{u}_y, \bar{u}_z]'$.
4) The predicted measurement is now $\hat{\mathbf{z}}_{k|k-1} = [\hat{z}_{k|k-1}^r, \hat{z}_{k|k-1}^\theta, \hat{z}_{k|k-1}^\phi]'$.

Similarly to how the differences in Section III-A for the polar coordinates are wrapped to the circle when computing $\mathbf{P}_{k|k-1}^{xz}$ and $\mathbf{P}_{k|k-1}^{zz}$ from (5) and (6) as well as the difference in (2), they will be wrapped to the sphere in this instance. To wrap the differences to the sphere, note that differences in azimuth and elevation can only vary in the range $(\pm\pi)$. However, if the elevations are limited to the range $\pm\pi/2$, then there will be no issues (i.e. with directional statistics) taking differences of points at the $\pm\pi/2$. Thus, it is assumed that all points are first wrapped such that the elevation is in the range $\pm\pi/2$. Though normally not an issue, Appendix B says how to perform this type of wrapping.

Thus (2) for spherical measurements becomes

$$\hat{\mathbf{x}}_{k|k} = \hat{\mathbf{x}}_{k|k-1} + \mathbf{P}_{k|k-1}^{xz}\left(\mathbf{P}_{k|k-1}^{zz}\right)^{-1} h_{\text{spher}}^{\text{wrap}}\left(\mathbf{z}_k - \hat{\mathbf{z}}_{k|k-1}\right), \tag{33}$$

where for some difference parameter $\Delta\mathbf{z} = [\Delta r, \Delta\theta]'$,

$$h_{\text{spher}}^{\text{wrap}}(\mathbf{z}) = \begin{bmatrix} r \\ h^{\text{wrap}}(\theta, -\pi, \pi) \\ \phi \end{bmatrix}. \tag{34}$$

The algorithm for finding $\mathbf{P}_{k|k-1}^{xz}$ and $\mathbf{P}_{k|k-1}^{zz}$ for spherical measurements is then very similar to the algorithm for the case with polar measurements:

1) Compute cubature points for the distribution of the predicted state in the manner normally done for cubature integration. That is, use (12) to get $\boldsymbol{\zeta}_i^z = [\zeta_i^{z,r}, \zeta_i^{z,\theta}, \zeta_i^{z,\phi}]'$ where $\zeta_i^{z,\phi} \in (\pm\pi/2)$. Normally, nothing extra has to be done to keep $\zeta_i^{z,\phi}$ in the proper range. Also, save the non-transformed cubature points,

$$\boldsymbol{\zeta}_i^x = \hat{\mathbf{x}}_{k|k-1} + \mathbf{P}_{k|k-1}^{\frac{1}{2}} \boldsymbol{\zeta}_i. \tag{35}$$

2) $\mathbf{P}_{k|k-1}^{xz}$ and $\mathbf{P}_{k|k-1}^{zz}$ are evaluated as

$$\mathbf{P}_{k|k-1}^{xz} = \sum_{i=0}^{N_C-1} \omega_i \left(\boldsymbol{\zeta}_i^x - \hat{\mathbf{x}}_{k|k-1}\right) h_{\text{spher}}^{\text{wrap}}\left(\boldsymbol{\zeta}_i^z - \hat{\mathbf{z}}_{k|k-1}, -\pi, \pi\right)', \tag{36}$$

$$\mathbf{P}_{k|k-1}^{zz} = \sum_{i=0}^{N_C-1} \omega_i h_{\text{spher}}^{\text{wrap}}\left(\boldsymbol{\zeta}_i^z - \hat{\mathbf{z}}_{k|k-1}\right) h_{\text{spher}}^{\text{wrap}}\left(\boldsymbol{\zeta}_i^z - \hat{\mathbf{z}}_{k|k-1}\right)'. \tag{37}$$

where for some difference parameter $\mathbf{z} = [r, \theta, \phi]'$,

B. An Example

To demonstrate the necessity and limitations of the wrapping algorithms four scenarios are considered, each differeing in the initialization used. The initializations are

$$\mathbf{x}_0^{(0)} = \begin{bmatrix} 100\,\text{km} & 0 & 0 & -200\,\text{m/s} & 0 & 0 \end{bmatrix}', \tag{38}$$

$$\mathbf{x}_0^{(1)} = \begin{bmatrix} -100\,\text{km} & 0 & 0 & 200\,\text{m/s} & 0 & 0 \end{bmatrix}', \tag{39}$$

$$\mathbf{x}_0^{(2)} = \begin{bmatrix} 0 & 0 & 100\,\text{km} & 0 & 0 & -200\,\text{m/s} \end{bmatrix}', \tag{40}$$

$$\mathbf{x}_0^{(3)} = \begin{bmatrix} a & 0 & a & b & 0 & b \end{bmatrix}', \tag{41}$$

where

$$a = \sqrt{\frac{(100)^2}{2}}\,\text{km} \qquad b = -\sqrt{\frac{200^2}{2}}\,\text{m/s}. \tag{42}$$

In all instances, the target starts at the same distance and speed, heading toward the origin. However, with $\mathbf{x}_0^{(0)}$, the target is far from the spherical poles and the $\pm\pi$ boundary in azimuth; in $\mathbf{x}_0^{(1)}$ it is near the $\pm\pi$ boundary in azimuth, but far from the poles; in $\mathbf{x}_0^{(2)}$ it is directly at the poles, and in $\mathbf{x}_0^{(3)}$, it is at a 45° elevation and far from the $\pm\pi$ boundary in azimuth.

The same dynamic model is used as in Section III-B, generalized to three dimensions, and range and azimuth and elevation standard deviations are respectively $\sigma_r = 20\,\text{m}$ and $\sigma_\theta = \sigma_\phi = 0.5^\circ$, which is the same range and azimuth accuracy as in Section III-B.

Figure 2 shows the RMSE performance of the four filters previously considered in the polar case, with the approximate BLUE filter for spherical coordinates taken from [38]. For the measurement conversion and cubature filters, the same fifth-order cubature points were used as in [9]. As expected, all of the filters have comparable performance in Scenario 0, which is far from any boundaries and is not plotted, but in 2a, near the azimuthal $\pm\pi$ boundary, the naive CKF performs very poorly. On the other hand, when the trajectory starts at 90° elevation in 2b, all of the filters except for the converted measurements Kalman filter perform very poorly. For the cubature filters, this can be explained by the fact that at exactly 90°, the azimuth coordinate provides no information, but the (linear) method of

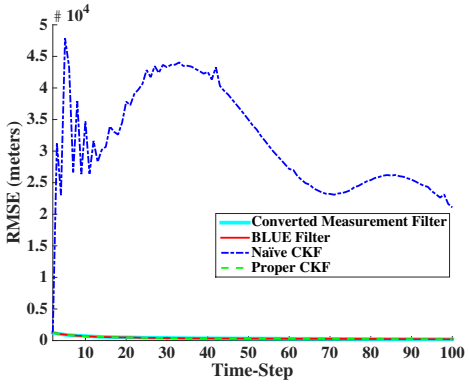

(a) Spherical Scenario 1: $\mathbf{x}_0^{(1)}$

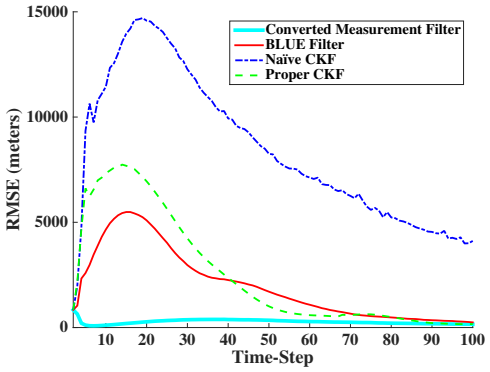

(b) Spherical Scenario 2: $\mathbf{x}_0^{(2)}$

Fig. 2. RMSE performance of the four filters under consideration when tracking in spherical coordinates. In Scenarios 0 and 3, the performance of all of the filters is similar and is not shown. In (a), the target is near the $\pm\pi$ boundary in azimuth. In (b), the target starts at 90° elevation and goes down towards the sensor.

computing the correlation matrices in (5) does not assign zero correlation terms due to artifacts of wrapping. In Scenario 3 (not plotted), the filters all appear to again be equivalent.

V. Conclusions

Corrections adapting CKFs to polar and spherical measurements were provided, eliminating extremely bad performance seen in certain regions with uncorrected filters. In the polar scenario, the corrected CKFs had similar performance when compared to an approximate BLUE estimator and were more consistent than using a converted-measurement Kalman filter. In the spherical scenario, the corrected CKF was found to be more consistent that the converted measurement filter or the BLUE at moderate elevation angles. With proper corrections for the circular nature of the components, the CKF can handle spherical and polar measurements arising from general ray-traceable measurement models as in [8], making the routine more generally applicable than the approximate BLUE estimators.

Acknowledgements

This research is supported by the Office of Naval Research through the Naval Research Laboratory (NRL) Base Program.

Appendix A
A General Discretized Nearly-Constant Linear Dynamic Model

The tutorial [7] discusses continuous-time stochastic dynamic model. A linear time-invariant stochastic dynamic model has the form

$$d\mathbf{x}_t = \mathbf{A}\mathbf{x}_t dt + \mathbf{D}d\mathbf{v}_t, \tag{43}$$

where $\mathbf{x}_t$ is the continuous-time state with differential $d\mathbf{x}_t$ (for a differential time increment dt), $d\mathbf{v}_t$ is the differential Wiener noise process, and $\mathbf{A}$ and $\mathbf{D}$ are constant matrices.

For one dimensional motion with an nth order model, with $n = 1$ being nearly constant velocity, $n = 2$, nearly constant position, and so on, the matrices are

$$\mathbf{A} = \begin{cases} 0 & \text{for } n = 0 \text{ (the scalar case)} \\ \begin{bmatrix} \mathbf{0}_{n,1} & \mathbf{I}_{n,n} \\ 0 & \mathbf{0}_{1,n} \end{bmatrix} & \text{for } n > 0 \end{cases} \tag{44}$$

$$\mathbf{D} = \begin{bmatrix} \mathbf{0}_{n,1} \\ 1 \end{bmatrix} q, \tag{45}$$

where q is the process noise intensity. The $\mathbf{A}$ matrix just integrates the moments upwards (velocity to position), and the $\mathbf{D}$ matrix injects noise into the model. This implies that $d\mathbf{v}_t$ is scalar.

The mathematics for discretizing such a system are described in [4, Ch. 6.2] and [31, Ch. 4.9]. If the interval between discrete-time step k and $k+1$ is T seconds, the discretized dynamic model simplifies to

$$\mathbf{x}_{k+1} = \mathbf{F}(T)\mathbf{x}_k + \mathbf{v}_k, \tag{46}$$

where the covariance matrix of the discrete-time noise is $\mathbf{Q}(T)$. The elements in row r and column c of the matrices $\mathbf{F}(T)$ and $\mathbf{Q}(T)$ are

$$[\mathbf{F}(T)]|_{r,c} = \begin{cases} \dfrac{T^{c-r}}{(c-r)!} & \text{if } c - r \geq 0 \\ 0 & \text{otherwise} \end{cases} \tag{47}$$

$$[\mathbf{Q}(T)]|_{r,c} = \frac{T^{(n-r)+(n-c)+1}}{(n-r)!(n-c)!((n-r)+(n-c)+1)} q^2. \tag{48}$$

To extend the model to multiple dimensions, multiple independent 1-dimensional dynamic models can be stacked. If the target state is should be in n-dimensional Cartesian space consisting of components $\mathbf{x} = [x_1, \ldots, \dot{x}_n, \dot{x}_1, \ldots, \dot{x}_n, \ddot{x}_1 \ldots]'$, where a dot above the variable represents a derivative, then

$$\mathbf{Q}^n(T) = \mathbf{Q}(T) \otimes \mathbf{I}_{n,n} \qquad \mathbf{F}^n(T) = \mathbf{F}(T) \otimes \mathbf{I}_{n,n}, \tag{49}$$

where $\mathbf{Q}^n(T)$ and $\mathbf{F}^n(T)$ are the process noise covariance matrix and state transition matrix for n-dimensions, $\mathbf{I}_{n,n}$ is the $n \times n$ identity matrix and $\otimes$ is the Kronecker product operator, which is the `kron` command in Matlab.

APPENDIX B
HOW TO WRAP WITH MIRRORING

Given a direction in spherical coordinates (θ, ϕ), where θ is azimuth and ϕ is elevation, but to which offsets have been added so that θ is no longer necessarily in the range of $\pm\pi$ radians and ϕ is no longer in the range $\pm\pi/2$ radians, the point can be mapped back to the sphere as follows:

If $\mod\left(\frac{\left(|\phi|-\frac{\pi}{2}\right)}{\pi}, 2\right) > 1$ then

$$\theta = h^{\text{wrap}}(\theta, -\pi, \pi) \qquad \phi = \arcsin(\sin(\phi)) \tag{50}$$

otherwise

$$\theta = h^{\text{wrap}}(\theta + \pi, -\pi, \pi) \qquad \phi = \arcsin(\sin(\phi)). \tag{51}$$

REFERENCES

[1] L. Angrisani, M. D'Apuzzo, and S. Lo Moriello, "Unscented transform: A powerful tool for measurement uncertainty evaluation," *IEEE Transactions on Instrumentation and Measurement*, vol. 55, no. 3, pp. 737–743, Jun. 2006.

[2] I. Arasaratnam and S. Haykin, "Cubature Kalman filters," *IEEE Transactions on Automatic Control*, vol. 54, no. 6, pp. 1254–1269, Jun. 2009.

[3] I. Arasaratnam, S. Haykin, and T. R. Hurd, "Cubature Kalman filtering for continuous-discrete systems," *IEEE Transactions on Signal Processing*, vol. 58, no. 10, pp. 4977–4993, Oct. 2010.

[4] Y. Bar-Shalom, X. R. Li, and T. Kirubarajan, *Estimation with Applications to Tracking and Navigation*. New York: John Wiley and Sons, Inc, 2001.

[5] L. Bruno, P. Braca, J. Horstmann, and M. Vespe, "Experimental evaluation of the range-Doppler coupling on HF surface wave radars," *IEEE Geoscience and Remote Sensing Letters*, vol. 10, no. 4, pp. 850–854, Jul. 2013.

[6] R. Cools, "An encyclopaedia of cubature formulas," *Journal of Complexity*, vol. 19, no. 3, pp. 445–453, Jun. 2003.

[7] D. F. Crouse, "Basic tracking using nonlinear continuous-time dynamic models," *IEEE Aerospace and Electronic Systems Magazine*, accepted, to Appear in 2015.

[8] ——, "Basic tracking using 3D monostatic and bistatic measurements in refractive environments," *IEEE Aerospace and Electronic Systems Magazine*, pp. 54–75, Aug. 2014.

[9] ——, "Basic tracking using nonlinear 3D monostatic and bistatic measurements," *IEEE Aerospace and Electronic Systems Magazine*, pp. 4–53, Aug. 2014.

[10] ——, "Maximum likelihood postdetection radar ambiguity resolution," *IEEE Transactions on Aerospace and Electronic Systems*, vol. 50, no. 3, pp. 1876–1883, Jul. 2014.

[11] D. F. Crouse, R. W. Osborne III, K. Pattipati, and Y. Bar-Shalom, "Efficient 2D sensor location estimation using targets of opportunity," *Journal of Advances in Information Fusion*, vol. 8, no. 1, pp. 73–89, Jun. 2013.

[12] Z. Ding and B. Balaji, "Comparison of unscented and cubature Kalman filters for radar tracking applications," in *Proceedings of the IET International Conference on Radar Systems*, Glasgow, UK, 22–25 Oct. 2012.

[13] N. Fisher, *Statistical Analysis of Circular Data*. Cambridge, UK: Cambridge University Press, 1993.

[14] N. Fisher, T. Lewis, and B. Embleton, *Statistical Analysis of Spherical Data*. Cambridge: Cambridge University Press, 1987.

[15] G. H. Golub and J. H. Welsh, "Calculation of Gauss quadrature rules," *Mathematics of Computation*, vol. 23, pp. 221–230, 1969.

[16] S. Julier, J. Uhlmann, and Durrant-Whyte, "A new method for the nonlinear transformation of means and covariances in filters and estimators," *IEEE Transactions on Automatic Control*, vol. 45, no. 3, pp. 477–482, Mar. 2000.

[17] S. J. Julier, "The scaled unscented transformation," in *Proceedings of the American Control Conference*, vol. 6, Anchorage, AK, 8–10 May 2002, pp. 4555–4559.

[18] ——, "The spherical simplex unscented transformation," in *Proceedings of the American Control Conference*, vol. 3, Denver, CO, 4–6 Jun. 2003, pp. 2430–2434.

[19] S. J. Julier and J. K. Uhlmann, "A consistent, debiased method for converting between polar and Cartesian coordinate systems," in *Proceedings of SPIE: Acquisition, Tracking, and Pointing XI*, vol. 3086, Orlando, FL, 23–24 Oct. 1997, pp. 110–121.

[20] ——, "A new extension of the Kalman filter to nonlinear systems," in *Proceedings of SPIE: Signal Processing, Sensor Fusion, and Target Recognition VI*, vol. 3068, Orlando, FL, 21 Apr. 1997, pp. 182–193.

[21] ——, "Unscented filtering and nonlinear estimation," *Proceedings of the IEEE*, vol. 92, no. 3, pp. 401–422, Mar. 2004.

[22] J. R. Katkuri, V. P. Jilkov, and X. R. Li, "A comparative study of nonlinear filters for target tracking in mixed coordinates," in *Proceedings of the 42nd South East Symposium on System Theory*, Tyler, TX, 7–9 Mar. 2010, pp. 202–207.

[23] G. Kurz, Gilitschenski, and U. D. Hanebeck, "Deterministic approximation of circular densities with symmetric Dirac mixtures based on two circular moments," in *Proceedings of the 17th International Conference on Information Fusion*, Salamanca, Spain, 7–10 Jul. 2014.

[24] G. Kurz, I. Gilitschenski, M. Dolgov, and U. Hanebeck, "Bivariate angular estimation under consideration of dependencies using directional statistics," in *Proceedings of the 53rd IEEE Conference on Decision and Control*, Los Angeles, CA, Dec. 2014.

[25] G. Kurz, I. Gilitschenski, and U. Hanebeck, "Recursive B—ayesian filtering in circular state spaces," Jan. 2015. [Online]. Available: http://arxiv.org/abs/1501.05151

[26] G. Kurz, I. Gilitschenski, and U. D. Hanebeck, "Nonlinear measurement update for estimation of angular systems based on circular distributions," in *Proceedings of the American Control Conference*, Portland, Oregon, 4–6 Jun. 2014, pp. 5694–5699.

[27] n. Lefebvre, TiBD02, H. Bruyninckx, and J. De Schutter, "Comment on "a new method for the nonlinear transformation of means and covariances in filters and estimators" (and author's reply)," *IEEE Transactions on Automatic Control*, vol. 47, no. 8, pp. 1406–1409, Aug. 2002.

[28] T. Lefebvre, H. Bruyninckx, and J. De Schutter, "Kalman filters for nonlinear systems: A comparison of performance," *International Journal of Control*, vol. 77, no. 7, pp. 639–653, 2004.

[29] X. R. Li and Z. Zhao, "Measuring estimator's credibility: Noncredibility index," in *Proceedings of the 9th International Conference on Information Fusion*, Florence, Italy, 10–13 Jul. 2006.

[30] K. V. Mardia and P. E. Jupp, *Directional Statistics*. Chichester, England: John Wiley & Sons, 2000.

[31] P. S. Maybeck, *Stochastic Models, Estimation, and Control*. New York: Academic Press, 1982, vol. 2.

[32] F. Sandblom and L. Svensson, "Marginalized sigma-point filtering," in *Proceedings of the 14th International Conference on Information Fusion*, Chicago, Illinois, 5–8 Jul. 2011.

[33] J. Steinbring and U. D. Hanebeck, "LRKF revisited: The smart sampling Kalman filter (S2KF)," *Journal of Advances in Information Fusion*, vol. 9, no. 2, pp. 106–123, Dec. 2014.

[34] O. Straka, J. Duník, and M. Šimandl, "Randomized unscented Kalman filter in target tracking," in *Proceedings of the 15th International Conference on Information Fusion*, Singapore, 9–12 Jul. 2012, pp. 503–510.

[35] A. H. Stroud, *Approximate Calculation of Multiple Integrals*. Edgewood Cliffs, NJ: Prentice-Hall, Inc., 1971.

[36] J. Traa and P. Smaragdis, "A wrapped Kalman filter for azimuthal speaker tracking," *IEEE Signal Processing Letters*, vol. 20, no. 12, pp. 1257–1260, Dec. 2013.

[37] United States Copyright Office. (2012, Jan.) How to investigate the copyright status of a work. [Online]. Available: http://www.copyright.gov/circs/circ22.pdf

[38] Z. Zhao, X. R. Li, and V. P. Jilkov, "Best linear unbiased filtering with nonlinear measurements for target tracking," *IEEE Transactions on Aerospace and Electronic Systems*, vol. 40, no. 4, pp. 1324–1336, Oct. 2004.